

Microscopic Study of (p,γ) Reactions in Mass Region $A=110-125$

Dipti Chakraborty,^{*} Saumi Dutta,[†] G. Gangopadhyay,[‡] and Abhijit Bhattacharyya[§]

*Department of Physics, University of Calcutta,
92 Acharya Prafulla Chandra Road, Kolkata-700009*

Low energy proton capture reactions have been studied in statistical model using the semi-microscopic optical potential in the mass range $A=110-125$. Nuclear density obtained from relativistic mean field calculation has been folded with nucleon-nucleon interaction to obtain the optical potential. Theoretical results have been compared with experimental measurements to normalize the potential. Results have also been compared with a standard calculation available in the literature.

PACS numbers: 24.10.Ht,25.40.Lw,25.40.Kv

Creation of nuclei heavier than iron occurs mainly through three processes - slow and rapid neutron capture processes and p-process [1–4]. Though some studies have shown that p-process amounts to only 0.1% of the total abundance of nuclei heavier than iron, there are possibly 35 isotopes on the neutron deficient side of valley of stability expected to be produced either entirely or partly through the p-process. The p-process depends on reactions such as (p,γ) , (γ,p) and (γ,n) reactions, as well as on the seed nuclei.

In spite of the high Coulomb barrier, various astrophysical sites may produce medium mass proton rich nuclei through radiative proton capture reaction with a huge proton flux. One of them is the x-ray burst where the peak temperature reaches 1-3 GK. In heavier nuclei, it is important to study the (γ,p) reactions which destroy proton rich nuclei and compete with the (γ,n) reactions. In terrestrial laboratories, it is easier to study (p,γ) reactions and infer the cross-sections for the inverse (γ,p) reactions. Besides, in astrophysical environments where photodisintegration occurs, the temperature is very high and nuclei are likely to exist in excited states as distinct from our laboratory experiments. Hence, the contribution of the ground state may not be substantial. All these arguments have led to the study of the forward (p,γ) reactions to constrain the rates.

To study the actual abundance of different nuclei and evolution of the process, a network calculation involving a large number of nuclear reactions is required. The network calculation in an explosive astrophysical situation has to take many quantities such as temperature, pressure, proton mass fraction, forward and inverse reaction rates etc in to account. Thus, we need to tune the interaction potential properly. As the p-process proceeds along proton rich side of the stability valley, it involves many nuclei which are unstable and inaccessible as targets on earth. Hence, theory remains the principal guide to gather information about various reactions. It is use-

ful to construct the nucleon-nucleus potential through folding of the NN interaction with the nuclear density. Nuclear density for stable targets may be experimentally measured by electron scattering. In unstable nuclei experimental nuclear densities are not available and theoretical results may be used.

Rauscher *et al.* [5, 6] have calculated the reaction rates for various proton, neutron and alpha induced reactions and their inverse reactions in Hauser-Feshbach formalism for various targets over wide ranges of atomic numbers, masses and temperatures in global approach. Optical potential, a key ingredient for Hauser-Feshbach calculation, is often taken in a local or global approach. In the present work we concentrate on the nuclei in the mass region $A=110-125$. There are a number of p-nuclei in and around this region, *viz.* ^{113}In , $^{112,114,115}\text{Sn}$, ^{120}Te and $^{124,126}\text{Xe}$. Away from the stability valley, reaction rates calculated even from semi-microscopic optical potential and phenomenological density prescription, become very uncertain and have to be varied by a large amount [7]. We have used a more microscopic approach where an appropriate microscopic NN interaction has been folded with nuclear density from mean field calculations to reduce this uncertainty. This process can be extended to the unstable nuclei. It is imperative to test the theoretical method in reactions where experimental data are available to verify its applicability before extending it to unknown isotopes. Hence, reaction cross-section for available stable targets in the mass region have been studied in the present work.

The density dependent M3Y interaction (DDM3Y), which is known to give satisfactory results in many cases, has been chosen for our purpose. Similar studies in mass region $A=55-100$ [8–12] have already been carried out and our aim is to extend this approach to $A=110-125$ region.

Energy being low in astrophysical environment, the nuclear skin plays a very important role in the nuclear reactions. In astrophysical situation nuclear reaction rate is sensitively dependent on nuclear density profile. Reliable density information can be obtained from relativistic mean field (RMF) theory, a very useful tool for explaining various low energy nuclear properties and nuclear structure as well as nuclear density [13, 14].

^{*}Electronic address: diptichakraborty2011@gmail.com

[†]Electronic address: saumidutta89@gmail.com

[‡]Electronic address: ggphy@caluniv.ac.in

[§]Electronic address: abhattacharyyacu@gmail.com

Nuclear density profiles have been calculated using the Lagrangian density FSU Gold [15]. This Lagrangian density contains, apart from the usual terms for nucleons and mesons, two additional non-linear meson-meson interaction terms, whose main role is to soften the EOS of symmetric matter and reduce the symmetry energy.

Calculation of density has been carried out in coordinate space assuming spherical symmetry. A pairing force of 300 MeV-fm for both protons and neutrons has been used under BCS approximation. More details for the method are available in Ref. [16]. Considering the finite size of the proton, charge density is obtained by convoluting the point proton density.

$$\rho_{ch}(\mathbf{r}) = e \int \rho(\mathbf{r}')g(\mathbf{r} - \mathbf{r}')d\mathbf{r}' \quad (1)$$

Here, $g(\vec{r})$ is the Gaussian form factor given by,

$$g(\vec{r}) = (a\sqrt{\pi})^{-3} \exp(-r^2/a^2) \quad (2)$$

where a is a constant whose value is assigned to be 0.8 fm.

It is well known that RMF can provide an excellent description of nuclear ground state properties in this mass region. To check the validity of nuclear density calculation, nuclear charge radii may be compared with measured values. In table I calculated binding energies and charge radii values have been compared with experimental measurements. The theoretical binding energy values have been corrected following the phenomenological procedure in Refs. [17, 18]. Here we have listed all the stable isotopes which occur in the concerned mass region and whose experimental charge radii values are known.

The relative difference between theoretical charge radii and experimental values is less than 0.5%. Binding energy values show a maximum error of 0.2%. Experimental binding energy and charge radii have been taken from Audi *et al.* [19] and Angeli [20], respectively. Effect of centre of mass correction would be small for heavy nuclei as relative correction in radius goes as $A^{-4/3}$, where A is the mass number of the nucleus [21].

The M3Y interaction [22, 23], even in absence of explicit density and energy dependence, is able to produce reasonably satisfactory results for processes like elastic scattering and reaction. After incorporation of density dependence, it is termed as density dependent M3Y (DDM3Y) interaction [24]. The effective nucleon-nucleon interaction incorporates the density term as

$$g(\rho, \epsilon) = C(1 - \beta(\epsilon)\rho^{2/3}) \quad (3)$$

ρ and ϵ are the nucleonic density and energy per nucleon, respectively. The constants C and β have been assigned to be 2.07 and 1.624 fm², respectively [25] obtained from optimum fit for α radioactivity data [26]. Here we also have used Scheerbaum spin orbit potential term [27] with phenomenological complex potential depths. The values used here for these phenomenological potential depths are same as in Refs. [8–11].

The DDM3Y interaction has been incorporated in TALYS1.4 code [28] for Hauser-Feshbach statistical model calculations. We have used the Goriely HFB-Skyrme calculations for theoretical nuclear masses in TALYS code for the nuclei whose experimental masses are not available. The prescriptions for level densities and gamma strength function are taken as Constant Temperature Fermi Gas model and Goriely's Hybrid model [29], respectively. All these features are available in the code. We have included the effect of the width fluctuation correction which has a significant impact at low incident energies. We have considered a maximum of 30 discrete levels in target nuclei and in residual nuclides. Full $j-l$ coupling has been used.

We have compared theoretical and experimental astrophysical S-factors. S-factor is a more slowly varying function of energy than the cross-section, and useful for comparison of results at very low energy.

The Gamow window for proton capture reaction is centered around the Gamow energy [30] in MeV

$$E_0 = 0.1220(Z_p^2 Z_t^2 \mu T_9^2)^{1/3} \quad (4)$$

with width in MeV

$$\Delta = 0.2368(Z_p^2 Z_t^2 \mu T_9^5)^{1/6} \quad (5)$$

Here, Z_p and Z_t are atomic numbers of the projectile and the target, μ is the reduced mass in a.m.u. of the system and T_9 is the temperature in GK. In the reactions considered in the present work Gamow window has a range from 1.8 to 4.5 MeV for temperature around 2-3 GK. Experimental masses have been taken from Ref. [19] in converting obtained reaction cross-section values to S-factor for comparison with experimental S-factor values. For (γ, p) reaction, it is worth noting that effective energy window will be centered at

$$E_\gamma^{eff} = E_0 + Q_{p\gamma} \quad (6)$$

because photodisintegration requires energy in excess of the threshold value, keeping the width unchanged.

In astrophysical environments temperature may be high and nuclei can exist in ground state as well as various excited states. Hence, Maxwellian averaging has been performed for reaction rates.

The optical potential has been normalized for the mass region considered to fit the experimental observations. The DDM3Y is a purely real interaction. We have chosen the real part of the potential by multiplying the folding potential with a factor 0.9. The imaginary part of the potential has been chosen identical with the real one. As we will show, it gives a reasonable agreement with the proton capture reactions in this mass region. Different normalizations for individual reactions may fit the observed data better for various reactions in this mass region. However, such a procedure will lead to a decrease in predictive power. In extending the calculation to unknown nuclei in the mass region, a single set of parameters will serve the purpose.

TABLE I: Calculated binding energy (MeV) and charge radii (fm) of nuclei in A=110-125 region compared with measured values.

Nucleus	Binding energy		Charge radius		Nucleus	Binding energy		Charge radius		Nucleus	Binding energy		Charge radius	
	Theory	Expt.	Theory	Expt.		Theory	Expt.	Theory	Expt.		Theory	Expt.	Theory	Expt.
^{110}Pd	939.78	940.21	4.552	4.578	^{112}Sn	952.46	953.53	4.609	4.594	^{124}Sn	1047.73	1049.96	4.695	4.676
^{110}Cd	939.24	940.64	4.575	4.574	^{114}Sn	970.64	971.57	4.622	4.610	^{121}Sb	1026.62	1026.32	4.690	4.680
^{111}Cd	947.98	947.62	4.581	4.580	^{115}Sn	979.14	979.12	4.630	4.617	^{123}Sb	1042.30	1042.10	4.704	4.688
^{112}Cd	956.38	957.01	4.588	4.595	^{116}Sn	987.24	988.68	4.638	4.627	^{122}Te	1033.75	1034.33	4.712	4.708
^{113}Cd	964.06	963.55	4.560	4.601	^{117}Sn	995.30	995.62	4.645	4.632	^{123}Te	1041.99	1041.26	4.719	4.711
^{114}Cd	971.82	972.60	4.604	4.614	^{118}Sn	1003.27	1004.95	4.653	4.641	^{124}Te	1050.13	1050.69	4.725	4.718
^{116}Cd	986.47	987.43	4.619	4.628	^{119}Sn	1010.96	1011.43	4.660	4.645	^{125}Te	1058.16	1057.26	4.732	4.720
^{113}In	963.88	963.09	4.605	4.602	^{120}Sn	1018.57	1020.54	4.667	4.654	^{124}Xe	1046.43	1046.26	4.755	4.762
^{115}In	980.06	979.40	4.621	4.617	^{122}Sn	1033.52	1035.52	4.681	4.666					

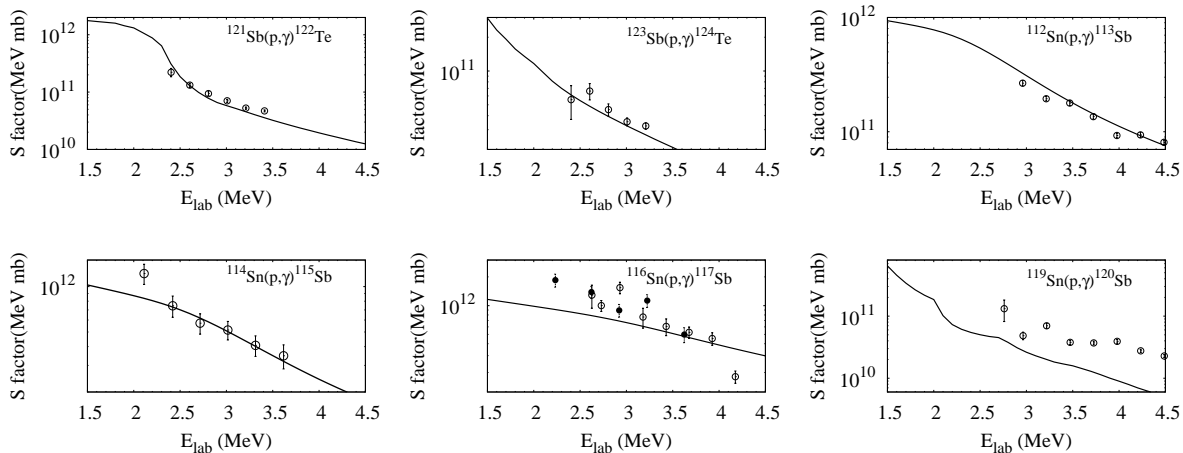


FIG. 1: Comparison of theoretical astrophysical S-factors with experimental data for the indicated proton capture reactions.

The comparison of S-factors for a number of reactions in this mass region are presented in Fig. 1. We have included all experimental work where reasonable amount of data exist. In all the figures solid lines denote the theoretical results. Open and solid circles with error bars denote experimental data. Experimental data for ^{121}Sb and ^{123}Sb have been taken from Harrisopulos *et al.* [31]. In that work experimental cross-sections were obtained from γ -angular distribution measurement with large volume HPGe detectors. Experimental data are from Chloupek *et al.* [32] for ^{112}Sn and ^{119}Sn , Famiano *et al.* [33] for ^{114}Sn and ^{116}Sn , and Ozkan *et al.* [34] for ^{116}Sn , respectively. Experimental data for ^{112}Sn and ^{119}Sn were obtained using activation technique with BGO detector and statistical model calculation was used to describe the results. For ^{114}Sn and ^{116}Sn activation technique was used to extract the cross-section [33].

One can see that the present method can describe the experimental results except in a few instances. Of course the errors are large in some cases. Except for the proton capture by ^{119}Sn , all the other reactions are reasonably described by the present procedure. It is worthwhile to note that statistical model calculations by the authors

failed to reproduce the cross sections for ^{119}Sn [32].

We have compared the astrophysical rates calculated using NON-SMOKER formalism [5, 6, 35] and our present calculation for reactions which involve p-nuclei as target or product to see how the present reaction rates differ from the standard ones available in the literature. In Fig. 2, we plot some of the rates where the differences between the two calculations are significant. The only exception is the $^{114}\text{In}(p, \gamma)$ reaction, which have been shown to emphasize that in some cases, the two methods agree to a great extent. The temperature T_9 is in GK. The data have been plotted in the temperature range 1.5 – 4 GK relevant to the above said Gamow window. We have used the NON-SMOKER results for astrophysical reaction rate data with Finite Range Droplet Model (FRDM) [36] nuclear masses for comparison. We find that our results are larger than the NON-SMOKER rates by a factor of 2-3 approximately in most cases. In some other reactions, the two results are very close to each other. It should be interesting to study the effect of the present rates on the p-process.

To summarize, a microscopic study of low energy (p, γ) reactions has been undertaken in the mass range A=110-

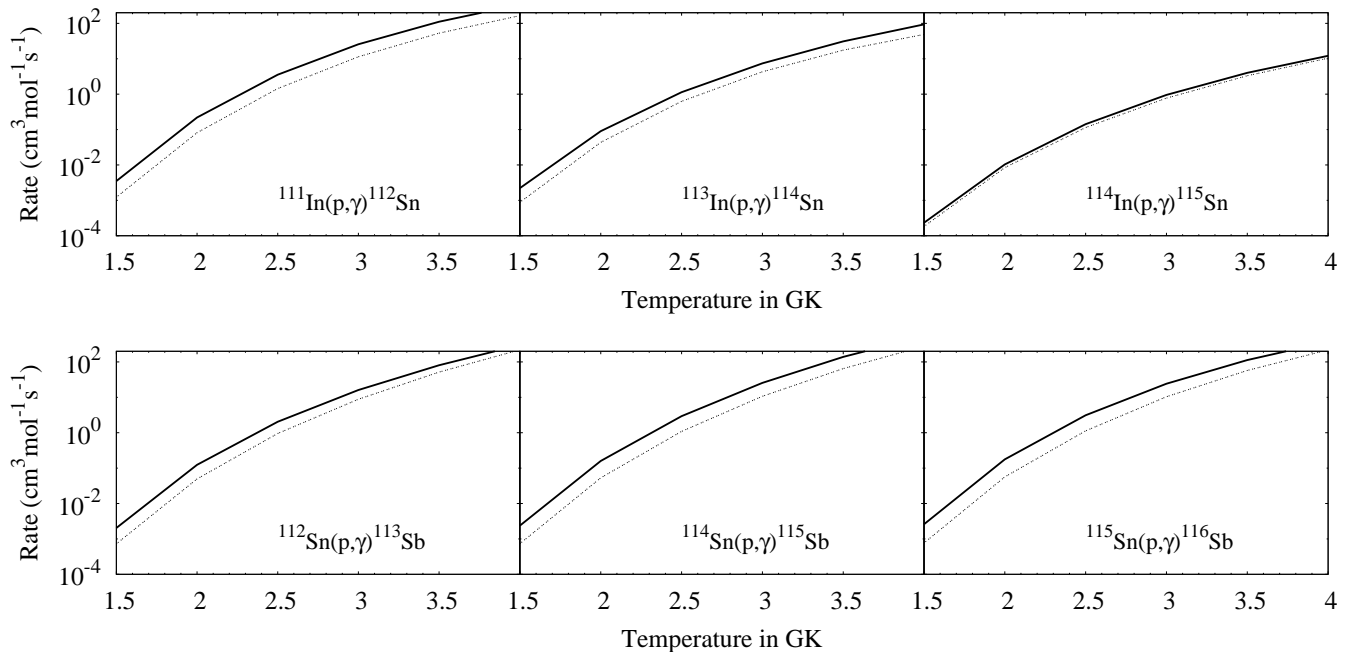


FIG. 2: Comparison of proton capture rates calculated from NON-SMOKER (dotted line) calculations and present work (solid line) for certain reactions involving p-nuclei.

125. RMF calculation has been performed to obtain the nuclear density profile. The real and imaginary parts of the optical model potential have been obtained by suitably normalizing the folding potential arising out of the DDM3Y interaction to explain the observed reaction data. S-factor values have been compared with experimental data. Proton capture reaction rates obtained

from our calculation have been compared with NON-SMOKER reaction rates.

The authors acknowledge the financial support provided by University Grants Commission, Department of Science and Technology, Alexander Von Humboldt Foundation and the University of Calcutta.

-
- [1] E. M. Burbidge, G. R. Burbidge, W. A. Fowler, and F. Hoyle, *Rev. Mod. Phys.* **29**, 547 (1957).
[2] F. Käppeler, R. Gallino, S. Bisterzo, and W. Aoki, *Rev. Mod. Phys.* **83**, 157 (2011).
[3] M. Arnould, S. Goriely, and K. Takahashi, *Phys. Rep.* **450**, 97 (2007).
[4] M. Arnould and S. Goriely, *Phys. Rep.* **384**, 1 (2003).
[5] T. Rauscher and F. -K. Thielemann, *At. Data Nucl. Data Tables* **75**, 1 (2000).
[6] T. Rauscher and F. -K. Thielemann, *At. Data Nucl. Data Tables* **76**, 47 (2001).
[7] H. Schatz, *Int. J. Mass Spec.* **251**, 293 (2006).
[8] G. Gangopadhyay, *Phys. Rev. C* **82**, 027603 (2010).
[9] C. Lahiri and G. Gangopadhyay, *Eur. Phys. J. A* **47**, 87 (2011).
[10] C. Lahiri and G. Gangopadhyay, *Phys. Rev. C* **84**, 057601 (2011).
[11] C. Lahiri and G. Gangopadhyay, *Phys. Rev. C* **86**, 047601 (2012).
[12] S. Dutta, D. Chakraborty, G. Gangopadhyay, and A. Bhattacharyya, *Phys. Rev. C* **91**, 025804 (2015). (2007).
[13] H. Muller and B.D. Serot, *Nucl. Phys. A* **606**, 508 (1996).
[14] P. Ring, *Prog. Part. Nucl. Phys.* **37**, 193 (1996).
[15] B. G. Todd-Rutel and J. Piekarewicz, *Phys. Rev. Lett.* **95**, 122501 (2005).
[16] M. Bhattacharya and G. Gangopadhyay, *Phys. Rev. C* **72**, 044318 (2005).
[17] M. Bhattacharya and G. Gangopadhyay, *Phys. Lett. B* **672**, 182 (2009).
[18] G. Gangopadhyay, *J. Phys. G* **37**, 015108 (2010).
[19] M. Wang, G. Audi, A. H. Wapstra, F. G. Kondev, M. MacCormick, X. Xu, and B. Pfeiffer, *Chin. Phys. C* **36**, 1603 (2012).
[20] I. Angeli, *At. Data Nucl. Data Tables* **87**, 185 (2004).
[21] P. Quentin, in *Nuclear Self-Consistent Fields*, edited by G. Ripka and M. Porneuf (North-Holland/ American Elsevier, 1975) p 297.
[22] G. Bertsch, J. Borysowicz, H. McManus, and W. G. Love, *Nucl. Phys. A* **284**, 399 (1977).
[23] G. R. Satchler and W. G. Love, *Phys. Rep.* **55**, 183 (1979).
[24] M. D. Myers, *Nucl. Phys. A* **204**, 465 (1973).
[25] D. N. Basu, P. Roy Chowdhury, and C. Samanta, *Phys. Rev. C* **72**, 051601 (2005).

- [26] D. N. Basu, J. Phys. G **30**, B7 (2004).
- [27] R. R. Scheerbaum, Nucl. Phys. A **257**, 77 (1976).
- [28] A. J. Koning, S. Hilaire, and M. Duizvestijn, Proceedings of the International Conference on Nuclear Data for Science and Technology, April 22-27, 2007, Nice, France, edited by O. Bersillon, F. Gunsing, E. Bauge, R. Jacqmin, S. Leray (EDP Sciences, 2008) p. 211.
- [29] S. Goriely, Phys. Lett. B **436**, 10 (1998).
- [30] C. E. Rolfs and W. S. Rodney, *Cauldrons in the Cosmos*, (The University of Chicago Press, Chicago and London, 1988).
- [31] S. Harissopulos, A. Spyrou, A. Lagoyannis, M. Axiotis, and P. Demetriou, Phys. Rev. C **87**, 025806 (2013).
- [32] F. R. Chloupek *et al.*, Nucl. Phys. A **652**, 391 (1999).
- [33] M. A. Famiano, R. S. Kodikara, B. M. Giacherio, V. G. Subramanian, and A. Kayani, Nucl. Phys. A **802**, 26 (2008).
- [34] N. Ozkan *et al.*, Nucl. Phys. A **710**, 469 (2002).
- [35] <http://nucastro.org/nonsmoker.html>.
- [36] J. R. Nix, W. D. Myers, and W. Swiatecki, At. Data Nucl. Data Tables **59**, 185 (1995).